Volatile loss under a diffusion-limited regime in tektites: Evidence from tin stable isotopes

John Creech, Frédéric Moynier, Christian Koeberl

Volatile loss under a diffusion-limited regime in tektites: evidence from tin stable isotopes

John B. Creech[1,2,*], Frédéric Moynier[1,3], and Christian Koeberl[4,5]

[1]*Institut de Physique du Globe de Paris, Université de Paris, 1 Rue Jussieu, 75328 Paris cedex 05, France*

[2]*Department of Earth and Planetary Sciences, Macquarie University, NSW 2109, Australia*

[3]*Institut Universitaire de France, 75005, Paris*

[4]*Department of Lithospheric Research, University of Vienna, Althanstrasse 14, 1090 Vienna, Austria*

[5]*Natural History Museum, Burgring 7, 1010 Vienna, Austria*

[*]*Email address: john.creech@mq.edu.au*

ABSTRACT

Tektites are glasses derived from near-surface continental crustal rocks that were molten and ejected from the Earth's surface during hypervelocity meteorite impacts. They are among the driest terrestrial samples, although the exact mechanism of water loss and the behaviour of other volatile species during these processes are debated. Based on the difference in magnitude of the Cu and Zn isotopic fractionations in tektites, and the difference of diffusivity between these elements, it was suggested that volatile loss was diffusion-limited. Tin is potentially well suited to testing this model, as it has a lower diffusivity in silicate melts than both Cu and Zn, but a similar volatility to Zn. Here, we analysed the Sn stable isotopic composition in a suite of seven tektites, representing three of the four known tektite strewn fields, for which Zn and Cu isotopes were previously reported. Tin is enriched in the heavier isotopes (≥2.5‰ on the $^{122}Sn/^{118}Sn$ ratio) in tektites, correlated with the degree of Sn elemental depletion in their respective samples as well as with Cu and Zn isotope ratios, implying a common control. While the isotope fractionation of Sn, Cu and Zn is a result of

volatility, the magnitude of isotope fractionation is strongly moderated by their relative rates of diffusion in the molten tektite droplets. An Australasian Muong Nong-type tektite analysed has the least Sn depletion and Sn isotope fractionation, consistent with these samples being more proximal to the source and experiencing a shorter time at high temperatures.

Keywords: tektites; volatiles; tin; stable isotopes; impacts

INTRODUCTION

Tektites are distal impact glasses, typically up to a few cm in size, formed by rapid melting of terrestrial upper crustal rocks during hypervelocity impacts on the Earth's surface (e.g., Shaw and Wasserburg, 1982; Koeberl, 1986, 1990, 1994; Koeberl et al., 1996; Melosh and Artemieva, 2004). Tektites have chemical and isotopic compositions similar to that of the terrestrial upper crust, and thus are thought to have formed by fusion of the target rocks/sediments rather than from the impactor itself (e.g., Shaw and Wasserburg, 1982; Koeberl, 1986, 1994).

Although tektites are generally chemically and isotopically similar to the upper crust, they are characterized by extremely low water contents (Beran and Koeberl, 2010; 0.002–0.02 wt.%; Koeberl, 1994), indicating a depletion of water (and potentially other volatiles) from their precursor rocks (typically sediments, with >1% water) while the tektites were molten. The mechanism for this depletion and, more broadly, the behaviour of volatile elements and molecules during tektite formation is not well understood. Volatilization is known to fractionate elemental and isotopic abundances of volatile elements, and isotopic fractionation of moderately volatile elements has been recorded, for example, in lunar samples (e.g., Cl, Ga, K, Zn, Rb; Sharp et al., 2010; Paniello et al., 2012; Kato et al., 2015; Boyce et al., 2015; Kato and Moynier, 2017; Pringle and Moynier, 2017; Wang and Jacobsen, 2016). Recently, even relatively refractory elements (e.g., Mg, Si, Ca, Ti) have been shown to have isotopic variations that are attributed to high-temperature volatility-related processes in the early Solar System (e.g., Richter et al., 2009; Pringle et al., 2014; Hin et al., 2017; Davis et al., 2018). As

such, developments of additional tools to investigate such processes are timely. Given that tektites were rapidly heated, molten, and quenched over timescales that are likely to capture kinetic effects related to volatility, stable isotopes of volatile elements are well-suited to studying tektite formation and the isotopic effects thereof.

So far, studies of isotopic fractionation in tektites have yielded equivocal results. Studies of Mg (Esat and Taylor, 1987, 1986), K (Herzog et al., 2008; Humayun and Koeberl, 2004; Jiang et al., 2019), B (Chaussidon and Koeberl, 1995), and Li (Magna et al., 2011) in tektites found that vapour fractionation (at least for those elements) did not play an important role during tektite formation, and that isotope ratios reflect the compositions of their source materials. However, those elements lie towards the more refractory end of the moderately volatile elements. Among the more volatile of the moderately volatile elements, Cd is enriched in the heavy isotopes in one Muong Nong-type Australasian tektite, which could reflect evaporative loss of light Cd isotopes (Wombacher et al. 2003), although with only one sample, this finding is inconclusive. Moynier et al. (2010, 2009) reported Zn and Cu isotope compositions, respectively, for a suite of tektites from all strewn fields. These results were reaffirmed by a study of moldavites and sediments of the Ries crater (Rodovská et al., 2017). Both Cu and Zn show significant isotopic fractionation that correlates with their elemental depletions, consistent with preferential evaporative loss of light isotopes (Moynier et al., 2010, 2009), and the larger isotopic fractionation in Cu was attributed to the greater chemical diffusivity of Cu over Zn due to their differences in ionic charge (i.e., Zn^{2+} vs. Cu^{+}; Moynier et al. 2010). However, this model is based on only two elements, and further testing is required to validate this hypothesis.

Tin is amongst the more volatile of the moderately volatile elements, and is potentially more volatile than both Cu and Zn. No quantitative estimates exist for the temperature of volatilization of these elements in conditions relevant to tektite formation. Cosmochemical condensation temperatures, based on condensation from a gas of solar nebular composition at

78 a partial pressure of ~10^{-4} atm. (Lodders, 2003), are often used as a first order estimate of
79 volatility. These would suggest the relative volatilities of these elements increase in the order
80 Cu << Zn ≲ Sn. Recent vaporization experiments of basalts at higher oxygen fugacities
81 suggest that the relative volatilities of these elements increase in the order Zn<Cu<Sn (Zn is
82 getting relatively less volatile under oxidizing conditions, while Sn stays the most volatile
83 element; Norris and Wood, 2017). However, another recent vaporization study under more
84 oxidising conditions suggests that Zn remains more volatile than Cu (Sossi et al., 2019),
85 although unfortunately Sossi et al. (2019) do not provide data for Sn. Here, we assume an
86 order of volatility is maintained under tektite forming conditions whereby Sn and Zn have
87 similar volatility, and Cu is less volatile than Sn and Zn.
88 Understanding the isotopic behaviour of Sn during evaporation will be central to
89 understanding isotopic data in planetary materials and in impact-related samples. Tin isotope
90 cosmochemistry is a new field, and so far, published data have been limited to conference
91 abstracts (Bourdon et al., 2017; Creech and Moynier, 2017; Fitoussi et al., 2017) and one
92 paper (Creech and Moynier, 2019). However, the discovery of a light isotopic composition of
93 Sn in lunar samples compared to the Earth (Fitoussi et al., 2017) is unique amongst isotopic
94 systems analysed so far. Tektites can be used as natural experiments to test the behaviour of
95 Sn during evaporation.
96 Here, we report the first Sn stable isotope data in a suite of tektites from three of the
97 four major tektite strewn fields in which Cu and Zn isotopic composition had been previously
98 reported (Moynier et al., 2009, 2010). We use these data to investigate the processes leading
99 to the chemical and isotopic compositions of tektites, and, in turn, the effect of volatility
100 related processes on the isotopic composition of tin. By comparing the isotope fractionations
101 of Cu, Zn, and Sn, as well as their relative diffusivities, we test the previous model of
102 Moynier et al. (2009) of volatile loss in a diffusion-limited regime. These constraints on the
103 isotopic behaviour of Sn during evaporation will be central to understanding isotopic data in

104 planetary materials and in impact-derived samples, and will assist in interpretation of future
105 analyses of other cosmochemical samples, such as lunar rocks and chondrites.

106 **MATERIALS AND METHODS**

107 **Sample descriptions**

108 The Sn isotopic composition of a total of seven tektites were analysed in this study,
109 comprising all samples from previous Zn and Cu work with sufficient remaining sample
110 material for Sn isotope analysis. Details of the samples are summarized in Table 1. These
111 tektite samples represent three of the four identified tektite strewn fields, comprising:

112 *Central European tektites*: Four moldavite tektites were studied, three of which are
113 from the vicinity of Jankov (Jankov 1, Jankov 2, Jankov 3) and one is from the vicinity of
114 Chlum (Chlum). Of these samples, three have been previously analysed for Zn isotope ratios
115 by Moynier et al. (2009), and three for Cu isotope ratios by Moynier et al. (2010) – see Table
116 1.

117 *North American tektites*: One North American tektite (BED 8402), which is from the
118 bediasite sub-strewn field (Texas). This sample has been previously described in Weinke and
119 Koeberl (1985), and analysed for Zn and Cu isotope ratios by Moynier et al. (2010, 2009).

120 *Australasian tektites*: Two Australasian tektites, both indochinites, were analysed in
121 this study. These comprise one Muong Nong type tektite from Thailand (MN 8309) and one
122 splash-form tektite from Hainan, China (HSF1). Both of the Australasian tektites have been
123 analysed for major and trace element compositions by Koeberl (1992) or Moynier et al.
124 (2009); Cu and Zn isotope data have also been published by Moynier et al. (2009, 2010).

125 For comparison with terrestrial compositions, isotopic and concentration data for four
126 commonly used USGS terrestrial reference materials are also given in Table 1. Note that in
127 the following discussion, a generic terrestrial upper crust $\delta^{122}/^{118}$Sn (the per mil deviation of
128 the ^{122}Sn/^{118}Sn ratio from the IPGP_Sn standard) composition is approximated as 0.00–
129 0.50‰, with [Sn] of 0.65–2.50 μg g^{-1}, based on data from Creech et al. (2017) and

Badullovich et al. (2017); the exact composition of the tektite source rocks may be further constrained in the future as Sn isotope data for more geological materials become available.

Analytical methods

Tin purification and isotopic analysis were conducted using the same methods as described by Creech et al. (2017; 2019). Powders comprising 55–380 mg of tektite samples were digested in a mixture of concentrated HF:HNO_3 in closed teflon beakers on a hotplate at 120 ˚C. Dissolved tektite samples were evaporated to incipient dryness at 100 ˚C, taken up in a small volume of concentrated HCl and dried down again before being taken up in 2 mL of 0.5 M HCl for loading on to columns. Biorad columns were prepared with 1.5 mL per column of TRU resin and cleaned prior to sample loading by repeated rinsing with 0.5 M HNO_3, 0.5 M HCl and milli-Q water. After loading, matrix was rinsed off the column with 4 mL of 0.5 M HCl and 7 mL of 0.25 M HCl, and Sn was subsequently eluted in 10 mL of 0.5 M HNO_3.

Prior to sample digestion, samples were doped with a ^{117}Sn–^{122}Sn double-spike to give approximate proportions of 40% Sn from the double-spike and 60% from the sample, as detailed by Creech et al. (2017). Tin stable isotope measurements were carried out using a Thermo-Scientific Neptune Plus MC-ICPMS at the Institut de Physique du Globe de Paris, France, under analytical conditions identical to those described by Creech et al. (2017). Isotope results are reported in $\delta^{122/118}Sn$ notation. Sufficient material was only available to measure each tektite sample once. Creech et al. (2017) reported an external reproducibility for this technique of (conservatively) ±0.065‰ on $\delta^{122/118}Sn$, or ca. 0.016‰ on a per amu basis. Uncertainties on figures represent either the internal error of the respective analysis or the external reproducibility, whichever is larger.

Data reduction was conducted offline using the freely available double-spike data reduction tool IsoSpike (www.isospike.org; Creech and Paul, 2015).

RESULTS

Tin isotopic and concentration data for tektites are presented in Table 1, along with literature data for Zn and Cu for the same tektite samples. Tektites are strongly fractionated towards heavy Sn isotopic compositions relative to those of terrestrial upper crust samples (Table 1; Fig. 1). Overall, the tektites span a range in $\delta^{122}/^{118}$Sn of ca. 2 ‰, which is significantly larger than any natural Sn isotopic variation so far reported for geological samples. The single North American tektite has a $\delta^{122/118}$Sn = 1.40 ± 0.18‰, whereas the Central European tektites span a range from $\delta^{122/118}$Sn = 1.35 ± 0.03‰ (Jankov 1) to 2.53 ± 0.15‰ (Chlum). The Australasian tektites are more variable; the splash form tektite from Hainan (HSF1) has a similar isotopic composition to the North American and Central European tektites ($\delta^{122/118}$Sn = 1.60 ± 0.10‰), while the Muong Nong-type tektite MN8309 is less fractionated, with a composition more similar to terrestrial upper crust ($\delta^{122/118}$Sn = 0.46 ± 0.18‰; basalt, Badullovich et al., 2017).

DISCUSSION

We observe a general shift towards heavy isotope compositions in tektites that is correlated with decreasing Sn content (Table 1, Fig. 1). This observation is consistent with evaporative loss of the light Sn isotopes during the molten phase of tektite formation, as previously observed for Cu and Zn (Moynier et al., 2010, 2009; Rodovská et al., 2017). In Figure 1 we show calculated isotopic compositions based on mass-dependent fractionation by Rayleigh distillation, which describes the isotopic evolution of a system from which a phase is continuously extracted. The isotopic composition of the tektites is well reproduced by a Rayleigh distillation, following a fractional distillation relationship for Sn as given in equation (1):

$$\frac{^{122}Sn/^{118}Sn}{^{122}Sn/^{118}Sn0} = \left(\frac{[Sn]}{[Sn]_0}\right)^{\alpha-1} \quad (1)$$

where α is the isotope fractionation factor, and the subscript 0 indicates initial values. The initial composition is an assumed terrestrial upper crust composition (note: on the scale of

isotopic fractionation observed in tektites, varying the initial composition within the range observed in terrestrial samples has little effect on the shape of projection, although it does change the relative position). In an ideal case, the kinetic fractionation factor, α, is dependent on the square root of the ratio of the masses involved (i.e., $\alpha_{ideal} = \sqrt{(M^{118}Sn/M^{122}Sn)}$, where $M^{118}Sn$ and $M^{122}Sn$ are the masses of ^{118}Sn and ^{122}Sn, respectively; in the case of Sn, $\alpha_{ideal} = 0.983$), although in natural samples fractionation factors are found to deviate from this ideal case (e.g., Moynier et al., 2009, 2010; Day and Moynier, 2014; Wimpenny et al., 2019). Suitable natural samples can thus be used to derive empirical kinetic fractionation factors that may be useful in interpreting volatility related isotope effects in other settings (with the caveat that additional factors/reactions may also affect isotopic fractionation). Tektites are well suited for this purpose.

As shown in Figure 1, the Sn isotopic compositions of most tektites are very close to predicted compositions from fractional distillation, for α values of 0.998 (Central European and North American tektites) or 0.999 (Australasian), and an initial composition of $\delta^{122/118}Sn_0 = 0.13‰$ and $[Sn]_0 = 1.6\ \mu g\ g^{-1}$. This match between observed and predicted isotope fractionation behaviour supports that during kinetic evaporation of a silicate melt the lighter isotopes of Sn are preferentially lost in the vapour.

The Muong Nong-type tektite MN8309 is closest in composition to terrestrial upper crust. This is consistent with previous observations that these tektites are less depleted in volatiles than splash form tektites, contain mineral remnants of the target, and were possibly deposited closer to the site of impact, having experienced lower formation temperatures (Glass and Barlow, 1979; Koeberl, 1994, 1992). Muong Nong-type tektites were also found to be less isotopically fractionated for Zn and Cu (Moynier et al., 2010, 2009). These results reflect the temperature–time regime (i.e., likely shorter periods of melting and evaporation) experienced by this group of tektites.

205 The Sn isotope data from tektites show strong correlations with Cu and Zn isotope
206 data (Table 1, Fig. 2). The correlations between these different isotope systems suggest that
207 they have been fractionated by a common process. Linear regressions through the data yield
208 R^2 values of 0.94 and 0.73 for Sn vs. Cu and vs. Zn, respectively (note that the moldavite
209 from Chlum appears to be an outlier in Cu isotope space, and was excluded from that
210 regression). Considering the similar relative mass differences of the respective isotope ratios
211 (i.e., 3.13% for $^{66}Zn/^{64}Zn$, 3.17% for $^{65}Cu/^{63}Cu$, and 3.39% for $^{122}Sn/^{118}Sn$), the slopes of the
212 regressions in Figure 1 represent the relative rate of isotope fractionation for each element,
213 which may result from e.g., volatility or diffusion rates, as discussed below. We find that the
214 rate of Sn isotope fractionation in tektites is ca. 94% that of Zn isotopes (i.e., not significantly
215 distinguishable within uncertainties), and ca. 17% that of Cu isotopes. If we assume
216 volatilities decrease as Sn ≥ Zn > Cu, as described above, this fractionation must be partially
217 moderated by another factor.
218 In the model of Moynier et al. (2010, 2009), molten tektite droplets are viscously
219 stirred, with differential evaporation occurring at the surface. While the evaporation is
220 controlled by volatility, the availability of elements at the surface for evaporation is governed
221 by the rate of diffusion, which depends on many factors (e.g., T, melt composition, ionic
222 radii). Where the diffusion rate of an element is slow, a diffusion-limited regime
223 predominates, and evaporative loss of the element is restricted. Thus, elements that diffuse
224 slowly in a melt are expected to be less isotopically fractionated, than elements that diffuse
225 quickly, and for a fixed evaporation flux, the relative isotopic fractionation between volatile
226 elements will be controlled by the diffusivity.
227 In anhydrous melts, the relative diffusivities of these elements increase in the order Sn
228 < Zn << K, Cu (Behrens and Hahn, 2009; Zhang et al., 2010; Yang et al., 2016; Ni et al.,
229 2017, 2018; see Supplementary Material for further discussion). Given the similar volatility
230 of Sn relative to Zn, the larger relative fractionation in Zn is therefore likely a consequence of

the slower diffusion of Sn in molten droplets. The relatively large isotope fractionation observed in Cu isotopes (Moynier et al., 2010), despite its lower volatility than Sn (and possibly Zn), is largely due to the greater availability of Cu resulting from the faster diffusion of Cu^+.

CONCLUSIONS

Tektites are enriched in the heavier isotopes of Sn, and the isotopic composition correlates with the degree of elemental Sn depletion in these samples. This is consistent with evaporative loss of light Sn isotopes in to the vapour phase during tektite formation. The observed Sn isotopic fractionation in tektites is consistent with calculations of fractional distillation of Sn, with corresponding kinetic fractionation factors (α) of ca. 0.998–0.999. A relationship is observed isotopic fractionation in Sn, Zn and Cu, suggesting a common fractionation process. The smaller relative isotopic fractionation of Sn compared to Zn, despite similar volatility, and the much larger isotopic fractionation of Cu reflects the availability of these elements at the droplet surface, which is limited by the rate of diffusion.

ACKNOWLEDGMENTS

We are grateful to three anonymous reviewers for their detailed and constructive comments on the manuscript, and to Don Porcelli for his editorial handling. F.M. acknowledges funding from the European Research Council [ERC Starting grant agreement 637503-Pristine] to as well as the financial support of the UnivEarthS Labex program at Sorbonne Paris Cité [ANR-10-LABX-0023 and ANR-11-IDEX-0005-02] and a chaire d'excellence ANR-Idex Sorbonne Paris Cité. We are grateful to three anonymous reviewers for constructive comments on an earlier version of this manuscript. Parts of this work were supported by IPGP multidisciplinary program PARI, and by Region île-de-France SESAME Grant no. 12015908.

REFERENCES

Badullovich, N., Moynier, F., Creech, J., Teng, F.-Z., Sossi, P.A., 2017. Tin isotopic fractionation during igneous differentiation and Earth's mantle composition. Geochemical Perspectives Letters 5, 24–28. https://doi.org/10.7185/geochemlet.1741

Behrens, H., Hahn, M., 2009. Trace element diffusion and viscous flow in potassium-rich trachytic and phonolitic melts. Chemical Geology, Experimental techniques for the study of hydrothermal fluids and silicate melts 259, 63–77. https://doi.org/10.1016/j.chemgeo.2008.10.014

Beran, A., Koeberl, C., 2010. Water in tektites and impact glasses by fourier-transformed infrared spectrometry. Meteoritics & Planetary Science 32, 211–216. https://doi.org/10.1111/j.1945-5100.1997.tb01260.x

Bourdon, B., Fitoussi, C., Wang, X., 2017. Isotope Fractionation during Partial Condensation, in: Goldschmidt 2017. Presented at the Goldschmidt, Paris, France.

Boyce, J.W., Treiman, A.H., Guan, Y., Ma, C., Eiler, J.M., Gross, J., Greenwood, J.P., Stolper, E.M., 2015. The chlorine isotope fingerprint of the lunar magma ocean. Science Advances 1, e1500380. https://doi.org/10.1126/sciadv.1500380

Chaussidon, M., Koeberl, C., 1995. Boron content and isotopic composition of tektites and impact glasses: Constraints on source regions. Geochimica et Cosmochimica Acta 59, 613–624. https://doi.org/10.1016/0016-7037(94)00368-V

Creech, J.B., Moynier, F., 2019. Tin and zinc stable isotope characterisation of chondrites and implications for early Solar System evolution. Chemical Geology 511, 81–90. https://doi.org/10.1016/j.chemgeo.2019.02.028

Creech, J.B., Moynier, F., 2017. Stable Isotope Fractionation of Sn during Planetary and Nebular Processes. Abstract, Goldschmidt 2017, Paris, France.

Creech, J.B., Moynier, F., Badullovich, N., 2017. Tin stable isotope analysis of geological materials by double-spike MC-ICPMS. Chemical Geology 457, 61–67. https://doi.org/10.1016/j.chemgeo.2017.03.013

Creech, J.B., Paul, B., 2015. IsoSpike: Improved Double-Spike Inversion Software. Geostandards and Geoanalytical Research 39, 7--15. https://doi.org/10.1111/j.1751-908X.2014.00276.x

Davis, A.M., Zhang, J., Greber, N.D., Hu, J., Tissot, F.L.H., Dauphas, N., 2018. Titanium isotopes and rare earth patterns in CAIs: Evidence for thermal processing and gas-dust decoupling in the protoplanetary disk. Geochimica et Cosmochimica Acta, Astrophysical Implications of Extraterrestrial Materials: A Special issue for Ernst K. Zinner 221, 275–295. https://doi.org/10.1016/j.gca.2017.07.032

Day, J.M.D., Moynier, F., 2014. Evaporative fractionation of volatile stable isotopes and their bearing on the origin of the Moon. Philosophical Transactions of the Royal Society of London A: Mathematical, Physical and Engineering Sciences 372, 20130259. https://doi.org/10.1098/rsta.2013.0259

Esat, T.M., Taylor, S.R., 1987. Mg Isotopic Composition of Microtektites and Flanged Australite Buttons. Abstract, Lunar and Planetary Science Conference 18, 267–268.

Esat, T.M., Taylor, S.R., 1986. Mg Isotope Composition of Ivory Coast Microtektites. Abstract, Lunar and Planetary Science Conference 17, 210–211.

Fitoussi, C., Wang, X., Bourdon, B., 2017. Tin Isotope constraints on the Formation of the Moon, in: Goldschmidt 2017. Abstract, Goldschmidt 2017, Paris, France.

Glass, B.P., Barlow, R.A., 1979. Mineral Inclusions in Muong Nong-Type Indochinites: Implications Concerning Parent Material and Process of Formation. Meteoritics 14, 55–67. https://doi.org/10.1111/j.1945-5100.1979.tb00479.x

Herzog, G.F., Alexander, C.M.O., Berger, E.L., Delaney, J.S., Glass, B.P., 2008. Potassium isotope abundances in Australasian tektites and microtektites. Meteoritics & Planetary Science 43, 1641–1657. https://doi.org/10.1111/j.1945-5100.2008.tb00634.x

Hin, R.C., Coath, C.D., Carter, P.J., Nimmo, F., Lai, Y.-J., Pogge von Strandmann, P.A.E., Willbold, M., Leinhardt, Z.M., Walter, M.J., Elliott, T., 2017. Magnesium isotope evidence that accretional vapour loss shapes planetary compositions. Nature 549, 511–515. https://doi.org/10.1038/nature23899

Humayun, M., Koeberl, C., 2004. Potassium isotopic composition of Australasian tektites. Meteoritics & Planetary Science 39, 1509–1516. https://doi.org/10.1111/j.1945-5100.2004.tb00125.x

Jiang, Y., Chen, H., Fegley, B., Lodders, K., Hsu, W., Jacobsen, S.B., Wang, K., 2019. Implications of K, Cu and Zn isotopes for the formation of tektites. Geochimica et Cosmochimica Acta 259, 170–187. https://doi.org/10.1016/j.gca.2019.06.003

Kato, C., Moynier, F., 2017. Gallium isotopic evidence for extensive volatile loss from the Moon during its formation. Science Advances 3, e1700571. https://doi.org/10.1126/sciadv.1700571

Kato, C., Moynier, F., Valdes, M.C., Dhaliwal, J.K., Day, J.M.D., 2015. Extensive volatile loss during formation and differentiation of the Moon. Nature Communications 6, 7617 EP. https://doi.org/10.1038/ncomms8617

Koeberl, C., 1994. Tektite origin by hypervelocity asteroidal or cometary impact: Target rocks, source craters, and mechanisms, in: Dressler, B.O., Grieve, R.A.F., Sharpton, V.L. (Eds.), Geological Society of America Special Papers, Large Meteorite Impacts and Planetary Evolution. Geological Society of America Special Paper 293, Boulder, Colorado, pp. 133–152.

Koeberl, C., 1992. Geochemistry and origin of Muong Nong-type tektites. Geochimica et Cosmochimica Acta 56, 1033–1064.

Koeberl, C., 1990. The geochemistry of tektites: an overview. Tectonophysics, Cryptoexplosions and catastrophes in the geological record, with a special focus on the Vredefort structure 171, 405–422. https://doi.org/10.1016/0040-1951(90)90113-M

Koeberl, C., 1986. Geochemistry of tektites and impact glasses. Annual Review of Earth and Planetary Sciences 14, 323–350.

Koeberl, C., Poag, C.W., Reimold, W.U., Brandt, D., 1996. Impact origin of the Chesapeake Bay Structure and the source of the North American tektites. Science 271, 1263–1266. https://doi.org/10.1126/science.271.5253.1263

Lodders, K., 2003. Solar System abundances and condensation temperatures of the elements. Astrophysical Journal 591, 1220–1247. https://doi.org/10.1086/375492

Magna, T., Deutsch, A., Mezger, K., Skála, R., Seitz, H.-M., Mizera, J., Řanda, Z., Adolph, L., 2011. Lithium in tektites and impact glasses: Implications for sources, histories and large impacts. Geochimica et Cosmochimica Acta 75, 2137–2158. https://doi.org/10.1016/j.gca.2011.01.032

Melosh, H.J., Artemieva, N., 2004. How Does Tektite Glass Lose Its Water? Presented at the Lunar and Planetary Science Conference.

Moynier, F., Beck, P., Jourdan, F., Yin, Q.-Z., Reimold, U., Koeberl, C., 2009. Isotopic fractionation of zinc in tektites. Earth and Planetary Science Letters 277, 482–489. https://doi.org/10.1016/j.epsl.2008.11.020

Moynier, F., Koeberl, C., Beck, P., Jourdan, F., Telouk, P., 2010. Isotopic fractionation of Cu in tektites. Geochimica et Cosmochimica Acta 74, 799–807. https://doi.org/10.1016/j.gca.2009.10.012

Ni, H., Shi, H., Zhang, L., Li, W.-C., Guo, X., Liang, T., 2018. Cu diffusivity in granitic melts with application to the formation of porphyry Cu deposits. Contributions to Mineralogy and Petrology 173, 50. https://doi.org/10.1007/s00410-018-1475-0

Ni, P., Zhang, Y., Simon, A., Gagnon, J., 2017. Cu and Fe diffusion in rhyolitic melts during chalcocite “dissolution”: Implications for porphyry ore deposits and tektites. American Mineralogist 102, 1287–1301. https://doi.org/10.2138/am-2017-5885

Norris, C.A., Wood, B.J., 2017. Earth’s volatile contents established by melting and vaporization. Nature 549, 507–510. https://doi.org/10.1038/nature23645

Paniello, R.C., Day, J.M.D., Moynier, F., 2012. Zinc isotopic evidence for the origin of the Moon. Nature 490, 376–379. https://doi.org/10.1038/nature11507

Pringle, E.A., Moynier, F., 2017. Rubidium isotopic composition of the Earth, meteorites, and the Moon: Evidence for the origin of volatile loss during planetary accretion. Earth and Planetary Science Letters 473, 62–70. https://doi.org/10.1016/j.epsl.2017.05.033

Pringle, E.A., Moynier, F., Savage, P.S., Badro, J., Barrat, J.-A., 2014. Silicon isotopes in angrites and volatile loss in planetesimals. Proceedings of the National Academy of Sciences 111, 17029–17032. https://doi.org/10.1073/pnas.1418889111

Richter, F., Dauphas, N., Teng, F.-Z., 2009. Non-traditional fractionation of non-traditional isotopes: Evaporation, chemical diffusion and Soret diffusion. Chemical Geology 258, 92–103. https://doi.org/10.1016/j.chemgeo.2008.06.011

Rodovská, Z., Magna, T., Žák, K., Kato, C., Savage, P.S., Moynier, F., Skála, R., Ježek, J., 2017. Implications for behavior of volatile elements during impacts—Zinc and copper systematics in sediments from the Ries impact structure and central European tektites. Meteoritics & Planetary Science 52, 2178–2192. https://doi.org/10.1111/maps.12922

Sharp, Z.D., Shearer, C.K., McKeegan, K.D., Barnes, J.D., Wang, Y.Q., 2010. The Chlorine Isotope Composition of the Moon and Implications for an Anhydrous Mantle. Science 329, 1050–1053. https://doi.org/10.1126/science.1192606

Shaw, H.F., Wasserburg, G.J., 1982. Age and provenance of the target materials for tektites and possible impactites as inferred from Sm-Nd and Rb-Sr systematics. Earth and Planetary Science Letters 60, 155–177. https://doi.org/10.1016/0012-821X(82)90001-2

Sossi, P. A., Klemme, S., O'Neill, H. St. C., Berndt, J., Moynier, F., 2019. Evaporation of moderately volatile elements from silicate melts: experiments and theory. Geochimica et Cosmochimica Acta 260, 204–231. https://dx.doi.org/ 10.1016/j.gca.2019.06.021

Wang, K., Jacobsen, S.B., 2016. Potassium isotopic evidence for a high-energy giant impact origin of the Moon. Nature 538, 487–490. https://doi.org/10.1038/nature19341

Weinke, H.H., Koeberl, C., 1985. Trace elements in two bediasite tektites. Meteoritics 20, 783.

Wimpenny, J., Marks, N., Knight, K., Rolison, J.M., Borg, L., Eppich, G., Badro, J., Ryerson, F.J., Sanborn, M., Huyskens, M.H., Yin, Q., 2019. Experimental determination of Zn isotope fractionation during evaporative loss at extreme temperatures. Geochimica et Cosmochimica Acta 259, 391–411. https://doi.org/10.1016/j.gca.2019.06.016

Wombacher, F., Rehkämper, M., Mezger, K., Münker, C., 2003. Stable isotope compositions of cadmium in geological materials and meteorites determined by multiple-collector ICPMS. Geochimica et Cosmochimica Acta 67, 4639–4654. https://doi.org/10.1016/S0016-7037(03)00389-2

Yang, Y., Zhang, Y., Simon, A., Ni, P., 2016. Cassiterite dissolution and Sn diffusion in silicate melts of variable water content. Chemical Geology 441, 162–176. https://doi.org/10.1016/j.chemgeo.2016.07.021

Zhang, Y., Ni, H., Chen, Y., 2010. Diffusion data in silicate melts. Reviews in Mineralogy and Geochemistry 72, 311–408.

FIGURE CAPTIONS

Figure 1. Sn isotopic composition versus Sn content in tektites, showing predicted isotopic fractionation (calculated using equation 1) from an initial terrestrial upper crust composition as Sn is lost from the reservoir. The different colour lines represent calculations using different hypothetical fractionation factors (i.e., α values), as indicated. The half-filled symbol indicates the Muong Nong type tektite, MN8309. Error bars reflect the internal error or the external reproducibility, whichever is larger. Where error bars are not visible, uncertainties are smaller than the data point.

Figure 2. Comparison between tektite data for Sn isotopes and a) Cu isotopes and b) Zn isotopes. Dashed lines represent linear regressions through the data, with R^2 values as indicated on the figure. The half-filled symbol indicates the Muong Nong type tektite, MN8309. The upper-most symbol indicates the moldavite Chlum, which was excluded from the linear regression on plot (a) as it is an outlier in both Cu and Sn isotope space. Error bars reflect the internal error or the external reproducibility, whichever is larger. Where error bars are not visible, uncertainties are smaller than the data point.

TABLE CAPTION

Table 1. Tin, Cu, and Zn isotopic and concentration data for tektites and USGS reference materials.

Table 1 footnote. Tin isotope and concentration data for USGS reference materials are from Creech et al. (2017). Zinc isotope data are from Moynier et al. (2009), with the exception of AGV-2, which is from Moynier et al. (2010), and all Zn isotope data are relative to JMC-Lyon. Copper isotope data from Moynier et al. (2010), with the exception of BCR-2 which is from Chen et al. (2016), and all Cu isotope data are relative to NIST SRM 976. Cu and Zn concentration data for USGS reference materials are GeoReM recommended values.

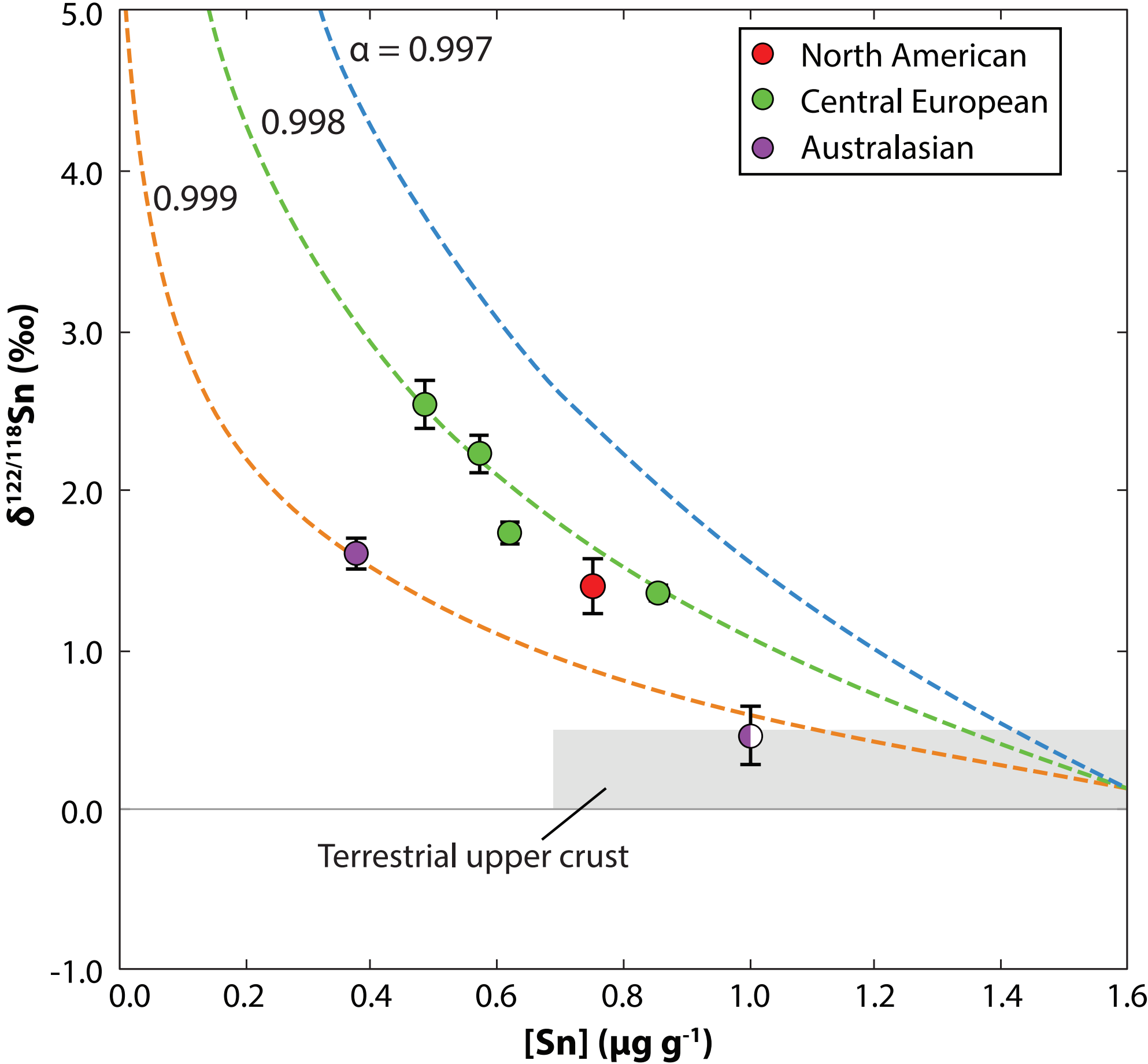
α = 0.997
0.998
0.999
North American
Central European
Australasian
Terrestrial upper crust
δ122/118Sn (‰)
[Sn] (µg g-1)
5.0
4.0
3.0
2.0
1.0
0.0
-1.0
0.0
0.2
0.4
0.6
0.8
1.0
1.2
1.4
1.6

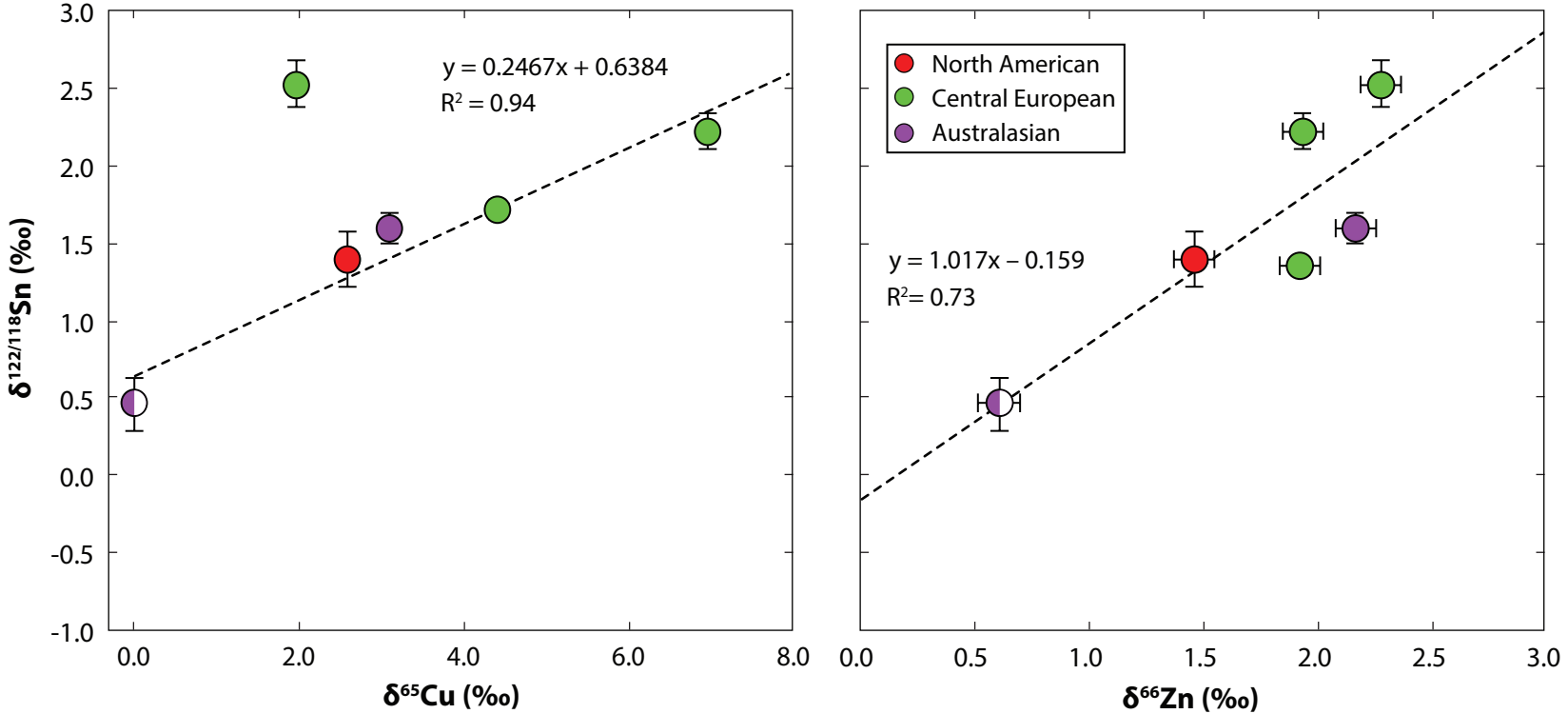
y = 0.2467x + 0.6384
R² = 0.94
δ122/118Sn (‰)
δ65Cu (‰)
North American
Central European
Australasian
y = 1.017x – 0.159
R²= 0.73
δ66Zn (‰)

Field	Type	Sample ID	$\delta^{122/118}$Sn (‰)	± (2 sd)	[Sn] (μg g^{-1})	$\delta^{65/63}$Cu (‰)	± (2 sd)	[Cu] (μg g^{-1})	$\delta^{66/64}$Zn (‰)	± (2 sd)	[Zn] (μg g^{-1})
North American	Bediasite	BED 8402	1.400	0.180	0.754	2.60	0.10	6.5	1.46	0.09	26
Central European	Moldavite	Jankov 1	1.352	0.028	0.853				1.92	0.09	29
Central European	Moldavite	Jankov 2	2.230	0.120	0.570	6.98	0.10	0.1	1.93	0.09	23
Central European	Moldavite	Jankov 3	1.725	0.051	0.619	4.41	0.10	0.1			24
Central European	Moldavite	Chlum	2.530	0.150	0.486	1.99	0.10	0.4	2.27	0.09	19
Australasian	Hainan	HSF1	1.600	0.100	0.379	3.11	0.10	2.2	2.16	0.09	8
Australasian	Muong Nong	MN8309	0.460	0.180	1.000	0.02	0.10	11.4	0.61	0.09	74
BHVO-2	Basalt		0.452	0.027	1.90	0.10	0.07	129.3	0.25	0.01	103.9
BCR-2	Basalt		0.404	0.650	2.36	0.20	0.09	19.7	0.27	0.06	129.5
GSP-2	Granodiorite		0.180	0.220	8.32			43.0			120.0
AGV-2	Andesite		0.310	0.120	2.07	0.10	0.11	51.5	0.25	0.09	86.7

n

Major element	Si	Al	Fe	Mg	Ca	Ti	K	Na	H2O	H2O Beran and Koeberl	Major element	SiO2	Al2O3	FeO	MgO	CaO	TiO2	K2O	Na2O
BED 8402			4.44	2.22	0.37	0.47		1.63	1.04	0.027		77.8	12.14	3.01	0.62	0.69	0.59	2.38	1.65
Jankov 1			5.54	1.34	1.17	1.78		3.01	0.35				0.529251	0.777305	0.603036	0.724691	0.599343	0.830148	0.741857
Jankov 2			5.2	1.3	1.52	2.29		2.85	0.31				6.43	2.34	0.37	0.50	0.35	1.98	1.22
Jankov 3																			
Chlum			3.84	1.17	1.49	2.45		2.39	0.2										
HSF1			4.41	2.81	0.93	1.15		1.79	0.82										
MN8309										0.024									

	SiO2	Al2O3	FeO	MgO	CaO	TiO2	K2O	Na2O	H2O	
BED 8402	77.8		8.39	2.86	0.61	0.65	0.59	1.96	1.40	0.027
Jankov 1			10.47	1.72	1.94	2.46		3.63	0.47	
Jankov 2			9.83	1.67	2.52	3.16		3.43	0.42	
Jankov 3										
Chlum			7.26	1.51	2.47	3.38		2.88	0.27	
HSF1			8.33	3.62	1.54	1.59		2.16	1.11	
MN8309										0.024

	0.529251	0.777305	0.603036	0.724691	0.599343	0.830148	0.741857

Weinke and K Moynier et al. ; Moynier et al. ; Moynier et al. ; Moynier et al. ; Weinke and K Moynier et al. ; Moynier et al. ; Beran and Koeberl (2010)

Field	Type	Sample ID	$\delta^{122/118}$Sn (‰)	± (2 sd)	[Sn] (µg g^{-1})	$\delta^{65/63}$Cu (‰)	± (2 sd)	[Cu] (µg g^{-1})	$\delta^{66/64}$Zn (‰)	± (2 sd)	[Zn] (µg g^{-1})
North American	Bediasite	BED 8402	1.400	0.180	0.754	2.60	0.10	6.5	1.46	0.09	26
Central Europear	Moldavite	Jankov 1	1.352	0.028	0.853				1.92	0.09	29
Central Europear	Moldavite	Jankov 2	2.230	0.120	0.570	6.98	0.10	0.1	1.93	0.09	23
Central Europear	Moldavite	Jankov 3	1.725	0.051	0.619	4.41	0.10	0.1			24
Central Europear	Moldavite	Chlum	2.530	0.150	0.486	1.99	0.10	0.4	2.27	0.09	19
Australasian	Hainan	HSF1	1.600	0.100	0.379	3.11	0.10	2.2	2.16	0.09	8
Australasian	Muong Nong	MN8309	0.460	0.180	1.000	0.02	0.10	11.4	0.61	0.09	74
BHVO-2	Basalt		0.452	0.027	1.90	0.10	0.07	129.3	0.25	0.01	103.9
BCR-2	Basalt		0.404	0.650	2.36	0.20	0.09	19.7	0.27	0.06	129.5
GSP-2	Granodiorite		0.180	0.220	8.32			43.0			120.0
AGV-2	Andesite		0.310	0.120	2.07	0.10	0.11	51.5	0.25	0.09	86.7